Redox Biology 58 (2022) 102544

Contents lists available at ScienceDirect

Redox Biology

journal homepage: www.elsevier.com/locate/redox

CPT1A promotes anoikis resistance in esophageal squamous cell carcinoma via redox homeostasis

Tian Tian [a,b,1], Yunxin Lu [a,1], Jinfei Lin [a,1], Miao Chen [a], Huijuan Qiu [a], Wancui Zhu [a], Haohui Sun [a], Jinsheng Huang [a,**], Han Yang [a,***], Wuguo Deng [a,*]

[a] Sun Yat-sen University Cancer Center, State Key Laboratory of Oncology in South China, Collaborative Innovation Center for Cancer Medicine, Guangzhou, 510060, Guangdong, China

[b] Department of Medical Biochemistry and Molecular Biology, School of Medicine, Jinan University, Guangzhou, 510632, Guangdong, China

ARTICLE INFO

Keywords:
CPT1A
Fatty acid oxidation
Anoikis resistance
Esophageal squamous cell carcinoma

ABSTRACT

Anoikis resistance was a prominent hallmark of cancer metastasis, and lipo-genic characteristics have been identified as another metabolic alteration during tumorigenesis. However, their crosstalk has not been fully elucidated, especially in advanced esophageal squamous cell carcinoma (ESCC). In this study, we showed, for the first time, that the key enzyme carnitine O-palmitoyl transferase 1 (CPT1A), which is involved in fatty acid oxidation (FAO), was markedly upregulated in ESCC cells upon detached culture via a metabolism PCR array. Overexpression of CPT1A was associated with poor survival of ESCC patients and could protect ESCC cells from apoptosis via maintaining redox homeostasis through supply of GSH and NADPH. Mechanistically, detached culture conditions enhanced the expression of the transcription factor ETV4 and suppressed the expression of the ubiquitin enzyme RNF2, which were responsible for the elevated expression of CPT1A at the mRNA and protein levels, respectively. Moreover, genetic or pharmacologic disruption of CPT1A switched off the NADPH supply and therefore prevented the anchorage-independent growth of ESCC cells *in vitro* and lung metastases of xenografted tumor models *in vivo*. Collectively, our results provide novel insights into how ESCC cancer cells exploit metabolic switching to form distant metastases and some evidence for the link between anoikis and FAO.

1. Introduction

Metastatic spreading often leads to a fatal outcome in cancer. Emerging evidence suggests that only subpopulations of primary cancer cells undergo multistep reprogramming to gain the ability to erode into the surroundings and evade apoptosis in the circulation could form metastatic lesions in distant organs [1]. All signals enabling metastatic cells to cope with extracellular stress and unfamiliar microenvironment may constitute, on the other hand, therapeutic vulnerabilities in cancer treatment [1,2]. Identifying vital nodes in metastatic networks would offer new opportunities to improve anticancer therapy beyond current strategies and eliminate both nodular lesions and cells during or even before metastatic transit.

The extracellular matrix (ECM) provides not only adhesion anchors for normal epithelial cells but also signals including proliferation, differentiation and apoptosis for maintaining organismal integrity [3]. Anoikis is defined as caspase-mediated apoptosis when cells are detached from the surrounding ECM(3). After leaving the primary lesions, the majority of malignant transformed cells will be eliminated by anoikis, but a small population can reprogram the extra and/or intrinsic signals to survive during the phases of invasion, circulation, and extravasation into the surrounding tissue, which is also known as anchorage-independent growth, and ultimately lead to the development of distant metastasis [1].

Metabolic modulation is one of the hallmarks of epithelial cells undergoing anoikis stress [3]. Upon detachment, malignant cells experience reduced glucose uptake and increased reactive oxygen species (ROS) levels, which pushes them toward anoikis [4,5]. Our previous report showed that AMPKα1 mediated phosphorylation of glutathione reductase is of vital to protect colorectal cancer cells from anoikis [6].

* Corresponding author. Sun Yat-Sen University Cancer center, Guangzhou, China.
** Corresponding author. Sun Yat-Sen University Cancer center, Guangzhou, China.;
*** Corresponding author. Sun Yat-Sen University Cancer center, Guangzhou, China.;
E-mail addresses: huangjsh@sysucc.org.cn (J. Huang), yanghan@sysucc.org.cn (H. Yang), dengwg@sysucc.org.cn (W. Deng).
[1] These authors contributed equally to this Article.

https://doi.org/10.1016/j.redox.2022.102544
Received 10 September 2022; Received in revised form 2 November 2022; Accepted 14 November 2022
Available online 15 November 2022

Moreover, we and others have provided evidence that cancer cells can rewire metabolic flow to generate NADPH via overexpression of key enzymes including G6PD, DGAT2 or MTHFD2 to circumvent elevated ROS when cultured in detached conditions [7–12].

Apart from generating metabolites including NADH and ATP to fuel cancer growth [13,14], fatty acid oxidation (FAO) could supply NADPH to protect cancer cells against environmental stresses, such as glucose deprivation or in detached conditions [5]. The rate-limiting step of FAO is the membrane transport of long-chain acyl-CoA from the cytoplasm to the inner mitochondrial matrix across the inner mitochondria by the carnitine palmitoyl transferase system (CPT), among which CPT1 is the key enzyme and CPT1A has been exploited as a possible therapeutic vulnerability [11,15,16]. Our previous work in colorectal cancer demonstrated that overexpression of CPT1A contributes to anchorage-independent survival and distant metastasis *in vitro* and *in vivo* [8]. However, few studies have focused on the roles of CPT1A in esophageal squamous cell carcinoma (ESCC) during anchorage-independent growth.

In this study, via a metabolism PCR array, we investigated the central metabolic reprogramming when ESCC cells were exposed to detached culture conditions and demonstrated that the expression of CPT1A was among the most markedly induced genes. Moreover, overexpression of CPT1A was correlated with a poor prognosis in ESCC patients. Genetic or pharmacological inhibition of CPT1A profoundly reversed anoikis resistance *in vitro* and *in vivo* by disrupting the NADPH supply to imbalance the redox homeostasis. In addition, we found that detachment could induce CPT1A upregulation via elevated transcription and reduced ubiquitination, which were mediated by increased expression of the transcription factor ETV4 and decreased expression of the ubiquitin enzyme RNF2, respectively. Our results revealed a critical function of CPT1A mediated FAO in anoikis resistance and indicated that CPT1A could be a novel therapeutic target in ESCC.

2. Materials and methods

2.1. Human tissue samples

A total of 281 ESCC tumor specimens and adjacent normal tissues from patients who underwent surgical resection at the Sun Yat-sen University Cancer Center (SYSUCC, Guangzhou, China) were formalin-fixed and paraffin-embedded (FFPE) and then stored. All patients provided written informed consent and assays used in our study were in accordance with our Institutional Review Board and the Declaration of Helsinki. In this cohort, 48 paired fresh samples were used for RNA extraction. Moreover, 81 paired tumor and metastatic lymph nodes and live metastases in the FFPE dataset were included. The clinicopathological characteristics of the patients whose samples are included are summarized in Supplementary Table S1 and Table S2.

2.2. Cell lines and reagents

NE-1 cells were obtained from American Type Culture Collection (ATCC, Rockville, MD, USA). K510, K150, K520, K410, and K180 cells were obtained from the German Cell Culture Collection (DSMZ, Braunschweig, Germany). TE-11, TE-9, and TE-15 cells were obtained from the Cell Bank of Shanghai Institute of Cell Biology (Chinese Academy of Medical Sciences, Shanghai, China). 293T cells were a kind gift from Professor Peng Huang (SYSUCC, Guangzhou, China). All cell lines were maintained in RPMI-1640 (HyClone, Logan, UT, USA) supplemented with 10% fetal bovine serum (Invitrogen, Carlsbad, CA, USA) and 1% penicillin/streptomycin (HyClone) at 37°C with 5% CO_2. Using short tandem repeat DNA profiling, all cells were authenticated by Guangzhou Cellcook Biotech Co., Ltd. (Guangzhou, China) to be excluded from the database of commonly misidentified cell lines and were shown to be mycoplasma-free. N-Acetyl-L-cysteine (NAC, A7250) was purchased from Sigma-Aldrich (St. Louis, MO, USA); perhexiline (S6959) was purchased from Selleck Chemicals (Houston, TX, USA).

2.3. RNA interference and plasmid transfection

Cell transfections and lentiviral transductions were performed according to our previous reports [17]. The small interfering RNAs (siRNAs) and plasmids overexpressing ETV4 were reported previously [17]. The short hairpin RNAs (shRNAs) for targeting and overexpressing CPT1A were the same as in our previous report [8]. ESCC cells were infected with lentiviruses containing 10 mg/ml polybrene and incubated with puromycin for 7 days. All the targeted sequences of siRNAs and shRNAs are summarized in Supplementary Table S3. For the plasmids, N-terminal HA-tagged CPT1A, ETV4 and luciferase reporter plasmids containing the CPT1A promoter were provided by Saisofi Biotechnology Co., Ltd (Jiangsu, China). The plasmids were transfected into the cells using Lipofectamine 3000 reagent (Invitrogen, Carlsbad, CA) according to the recommended protocol.

2.4. Western blot, qPCR analysis and immunohistochemical (IHC) staining analysis

Western blot analysis was performed according to our previous reports [7,8,17]. Briefly, the proteins from cells or tissues were extracted using RIPA buffer, quantified with a BCA assay kit (Thermo Fisher Scientific, Carlsbad, CA, USA) and immunoblotted after SDS-PAGE. The antibodies used in this study, including anti-CPT1A (ab128568), anti-RNF2 (ab181140), anti-FBXO6 (ab153853), anti-KBTBD7 (ab230126), anti-HERC2 (ab85832), anti-HUWE1 (ab271032) and anti-CACYBP (ab171972) were from Abcam (Cambridge, MA, USA); anti-pan-ubiquitin (20326), anti-β-Actin (4970) and anti-HA-tag (2367) were from Cell Signaling Technology (Beverly, MA, USA); anti-ETV4 (ARP32263_P050) was from Aviva Systems Biology (San Diego, CA, USA). RNA levels were measured by qPCR analysis according to the manufacturer's instructions and the primer sequences are listed in Supplementary Table S4. Samples collected to evaluate the expression of CPT1A, ETV4 and RNF2 were analyzed immunohistochemically according to a previously described method [17].

2.5. Microarray analysis

The NuRNA™ Human Central Metabolism PCR Array (Arraystar Inc., MD, USA) was used to identify dysregulated transcripts in ESCC cells cultured in normal and detached conditions. A total of 373 key enzymes involved in cancer metabolism were included in this array, as in our previous report [8].

2.6. Measurement of anoikis and sphere formation assays

ESCC cells cultured in ultralow attachment plates mimicking the matrix detachment conditions were harvested and collected to produce a single-cell suspension. For anoikis measurement, cells were stained with an Annexin V-FITC and PI kit (KeyGEN, Nanjing, China) before measurement with flow cytometer.

For anchorage-independent growth, 2×10^3 cells were plated in 96-well ultralow attachment plates (7007, Corning) with serum-free DMEM-F12 medium with 20 ng/ml epidermal growth factor (EGF) (100-47, Peprotech), 20 ng/ml basic fibroblast growth factor (bFGF) (100-18B, Peprotech), 10 μg/ml heparin (H3149, Sigma), and 2% B27 (17504044, Gibco). Then, spheres greater than 50 μm in diameter in each well were counted under a microscope after 7 days.

2.7. Measurement of ROS, NADPH/NADP+, GSH/GSSG and CPT1A activity

Measurement of intracellular ROS levels was performed as described previously [6]. Briefly, cells cultured in matrix detachment plates were

incubated with 10 mmol/L H2-DCFDA (Thermo Fisher Scientific) for 30 min, collected in ice-cold PBS, resuspended, and immediately measured in a flow cytometer (Beckman-Coulter). Intracellular NADPH/NADP + and GSH/GSSG were determined with different kits from Promega according to the manufacturer's instructions. The activity of CPT1A was measured as previously reported [18].

2.8. Reporter assay and chromatin immunoprecipitation assay

The dual reporter construct containing the human CPT1A promoter and luciferase was from GeneCopoeia, Inc. After transfection with the indicated plasmids or siRNAs, the luciferase activity was measured according to the manufacturer's instructions (GeneCopoeia, Inc.) and normalized to that of the internal control. The chromatin immunoprecipitation (ChIP) assay was performed with an EZ-Chip Kit (Millipore) following the manufacturer's instructions as described previously [17].

2.9. In vivo metastasis and therapeutic assay

ESCC cells (2×10^6) expressing shCtrl or shCPT1A were injected via the tail vein in female BABL/c nude mice (3–4 weeks old) purchased from Beijing Vital River Laboratory Animal Technology Co., Ltd. After six weeks, the mice were euthanized and the lungs were excised. All micrometastases were examined using a dissecting microscope after staining with hematoxylin–eosin.

To investigate the antitumor effects of perhexiline alone or in combination with oxaliplatin, K180 and K510 cells were injected via the tail vein. All mice were assigned randomly one week later to receive perhexiline (8 mg/kg every other day) or PBS at the same dose. The mice were weighed every five days and the survival times were recorded. Approximately six weeks after treatment, all the mice were killed, and lung metastases were recorded. The animal study was approved by the Institutional Animal Care and Use Committee of Sun Yat-Sen University.

2.10. Statistical analysis

All data provided are presented as the mean ± SD. All experiments were repeated at least three times. Statistical analysis was performed using GraphPad Prism 6 (San Diego, CA, USA) and the SPSS software package (version 13.0, SPSS Inc.). Student's *t*-test (paired or unpaired, two-tailed) and the chi-square test were used as appropriate, and *P* values less than 0.05 were considered significant.

3. Results

3.1. CPT1A was induced by detachment in culture and overexpressed in ESCC

As metabolic rewiring in ESCC during detachment were elusive, TE11, K150 and K510 cells cultured in attached and detached conditions were subjected to a PCR array containing key metabolic enzymes (Fig. 1A). Dysregulated genes were analyzed via bioinformatic methods, and seven genes (AMT, CPT1A, SLC2A2, SLC16A8, MDH1B, LDH1L6B, CEL) were found to be consistently upregulated (Fig. 1B and S1A). The qPCR results showed that CPT1A was the most upregulated gene (Fig. S1B) and western blotting results validated that upon detachment, the expression of CPT1A was elevated in a time-dependent manner in TE11, K510 and K510 cells (Fig. 1C). We then chose CPT1A for further investigation. CPT1A was also found to be upregulated in tumor tissues compared with normal counterparts as well as in liver metastases compared with paired primary tumors when assessed via qPCR in fresh samples collected at our institute (Fig. 1D). Moreover, overexpression of CPT1A was validated in the Oncomine database (Fig. 1E). We then assessed the expression of CPT1A via IHC in ESCC tumors, lymph nodes and liver metastases (Fig. 1F). Fig. 1G shows consistent overexpression of CPT1A in tumor tissues, metastatic lymph nodes and distant metastatic lesions when compared with paired adjacent normal tissues and primary tumors. In the univariate and multivariate analyses, overexpression of CPT1A was associated with poor overall and disease-free survival in ESCC (Fig. 1H and Supplementary Table S2). Collectively, CPT1A was induced by detached culture conditions and overexpressed in ESCC, especially in metastatic lesions, which predicted poor survival.

3.2. Knockdown of CPT1A induced anoikis and suppressed anchorage-independent growth

To explore the roles of CPT1A in metastasis in-depth, we first assessed CPT1A expression in a panel of ESCC cells (Fig. 2A). K180 and K510 cells, with relatively high CPT1A expression, were used to construct knockdown cell lines, which were validated by western blotting (Fig. 2B). Knockdown of CPT1A induced a significant percentage of apoptosis in K180 and K510 cells when cultured in detached conditions, while cells cultured in normal conditions remained alive regardless of CPT1A expression (Fig. 2C and D). Furthermore, anchorage-independent growth, indicated by sphere numbers forming in detached culture medium, was significantly suppressed upon CPT1A knockdown in K180 and K510 cells (Fig. 2E and F). Finally, we overexpressed CPT1A in the relatively low-expressing K150 and TE15 cells (Fig. 2G). Overexpression of CPT1A significantly inhibited cell death (Fig. 2H) and promoted sphere formation under detachment conditions (Fig. 2I). In summary, CPT1A was required for ESCC cells to survival upon detachment stress.

3.3. Knockdown of CPT1A aggravated detachment induced redox stress

To further explore metabolic alterations upon detachment and CPT1A knockdown, the DCF-DA probe was used to quantify the intracellular ROS level. Fig. 3A shows significantly elevated ROS levels in K180 and K510 cells cultured in detached conditions compared with attached cells (Fig. 3A). Moreover, knockdown of CPT1A further promoted ROS levels in K180 and K510 cells (Fig. 3A and B). NADPH and GSH were recognized as the major players in the antioxidant system and were tested in K180 and K510 cells. Although the NADPH/NADP + ratio was slightly reduced in attached K180 and K510 cells after knockdown of CPT1A, a remarkable decrease was observed in detached conditions (Fig. 3C). The ratio between GSH and GSSG showed similar tendency to that of NADPH/NADP+ (Fig. 3D). Moreover, cell apoptosis (Fig. 3E) and anchorage-independent growth (Fig. 3F and G) induced by knockdown of CPT1A upon detachment were rescued by treatment with the antioxidant NAC, further demonstrating the vital protective roles of CPT1A mediated redox homeostasis upon detachment stress.

3.4. ETV4 promoted the expression of CTP1A at the transcriptional level

Overexpression of CPT1A has been reported in several solid tumors [8,14,15], but the precise mechanisms remain to be explored. We found that the transcription factor ETV4 was responsible for ME1 overexpression in gastric cancer [17]. However, its role in ESCC has not been reported. Via analysis of TCGA-ESCC data, a positive correlation between ETV4 and CPT1A was observed (Fig. 4A) and two putative ETV4 binding sites were found in the CPT1A promotor (Fig. 4B). Subsequent ChIP-qPCR assays indicated that both binding elements were significantly enriched in the ETV4 immunoprecipitants (Fig. 4C). Dual-luciferase reporter assays further validated that knockdown of ETV4 suppressed the luciferase activity of K180 and K510 cells transfected with a CPT1A promotor (Fig. 4D), while overexpression of ETV4 stimulated the luciferase activity (Fig. 4E). In addition, siRNA mediated knockdown of ETV4 resulted in decreased expression of CPT1A at both the mRNA (Fig. 4F) and protein level (Fig. 4G). However, detachment induced ETV4 and CPT1A overexpression was blocked by addition of NAC (Fig. 4H), indicating that ROS may make a difference in this condition. Finally, the expression of ETV4 and CPT1A was assessed in our

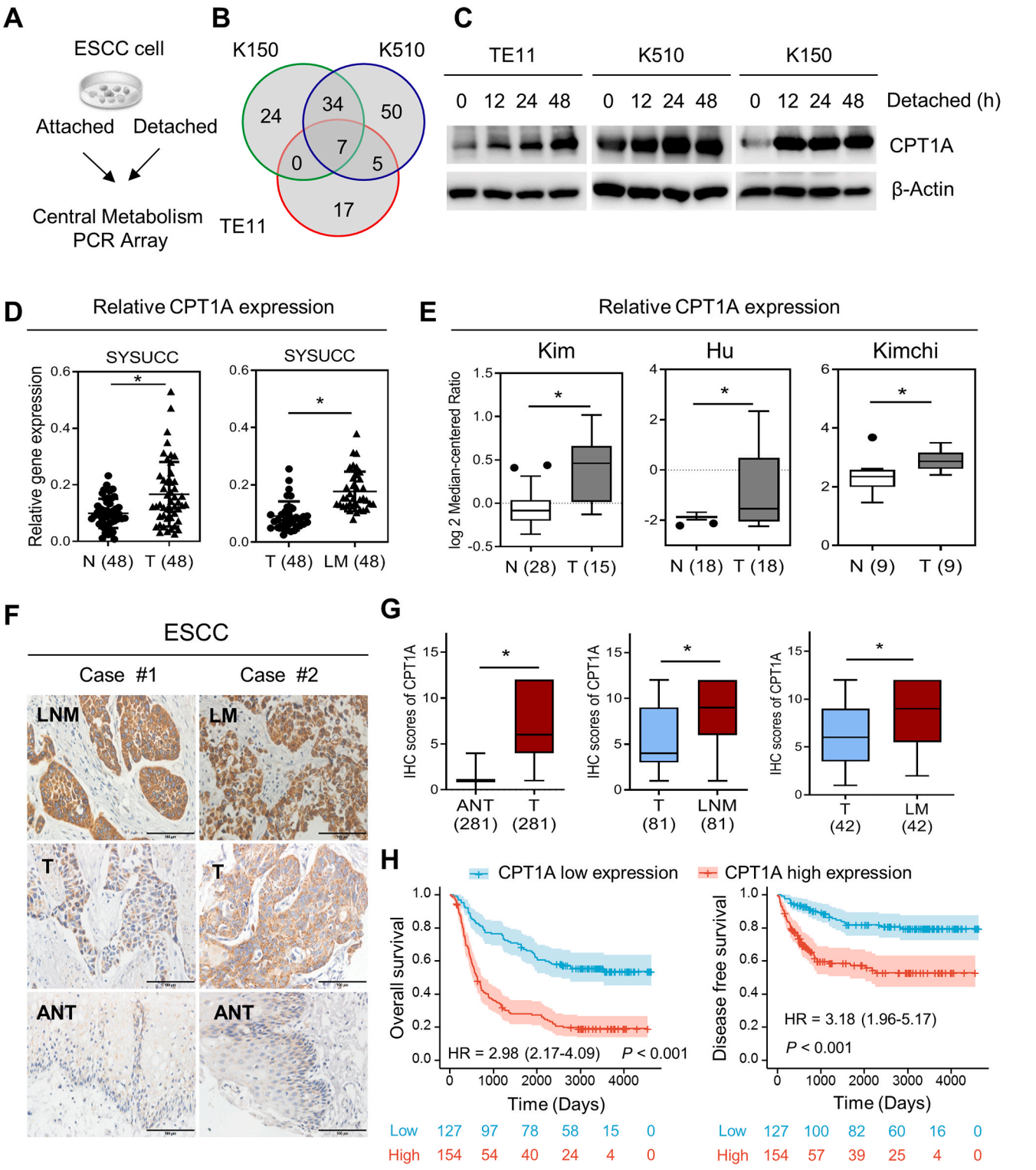

Fig. 1. CPT1A was induced in ESCC cells upon detachment stress and overexpressed in ESCC clinical samples. **A.** Diagram showing the strategy of the central metabolism PCR array screen with attached and detached ESCC cells. **B.** Venn diagram illustrating the enriched genes in the detached groups compared with the attached groups in K150, K510 and TE11 cells. **C.** Western blot analysis of CPT1A expression in K510, TE11 and K150 cells after detached culture for 12 h, 24 h and 48h. **D.** qPCR detection of *CPT1A* mRNA expression in 48 pairs of primary ESCC tumor tissues (T) and adjacent normal tissues (N) (left); 48 pairs of liver metastases (LM) (right) from SYSUCC. **E.** The relative mRNA levels of *CPT1A* in ESCC tumor tissues compared with normal tissues from the Oncomine database. **F, G.** Representative IHC staining images of CPT1A. Scale bar = 100 μm (**F**); the IHC staining scores of CPT1A expression in paired primary ESCC tumor tissues (N = 281), lymph node metastatic tissues (LNM, N = 81), or liver metastases (LM, N = 42) from SYSUCC (**G**). **H.** Overall survival or disease-free survival assays for ESCC patients with low vs. high expression of CPT1A based on IHC staining scores. β-Actin was included as a loading control. Data in **E** and **G** are presented as a box-and-whiskers graph (min-max), and the horizontal line across each box indicates the median. The *P* values in **D, E, G** were calculated using two-sided paired or unpaired Student's *t*-test. **H** was using Kaplan-Meier analysis with the log-rank test. $^{*}P < 0.05$.

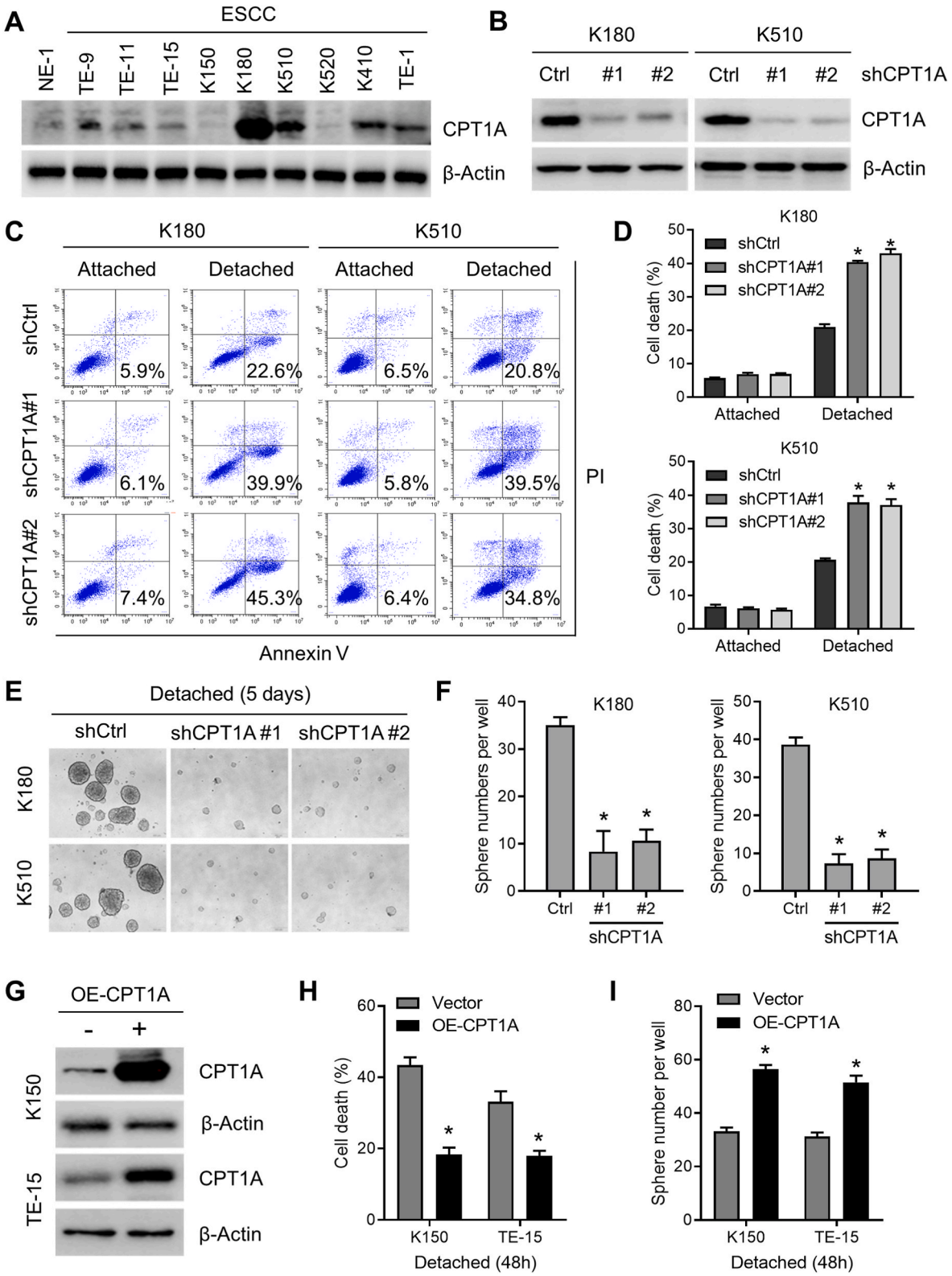

Fig. 2. Knockdown of CPT1A induced anoikis and suppressed anchorage independent growth of ESCC cells. **A, B.** Western blot analysis of CPT1A expression in a panel of human ESCC cells and normal esophageal epithelial cells (NE-1) (**A**) and control or CPT1A-knockdown K180 and K510 cells (**B**). **C, D.** Flow cytometry (**C**) and quantification analysis (**D**) with Annexin V/PI staining in control or CPT1A-knockdown K180 and K510 cells after attached or detached culture for 48 h. **E, F.** Sphere formation (**E**) and quantification analysis (**F**) in control or CPT1A-knockdown K180 and K510 cells after attached or detached culture for 5 days. **G.** Western blot analysis of CPT1A expression in CPT1A overexpressing K150 and TE-15 cells. **H, I.** Quantification analysis of the percentage of dead cells (**H**) and sphere formation number (**I**) in control and CPT1A-overexpressing K150 and TE-15 cells after detach culture for 48 h and 5 days. β-Actin was included as a loading control. Data in **D, F, H,** and **I** are representative of three independent experiments and presented as the mean ± S.D. The *P* values in **D, F, H,** and **I** were calculated using two-sided unpaired Student's *t*-test. $^*P < 0.05$.

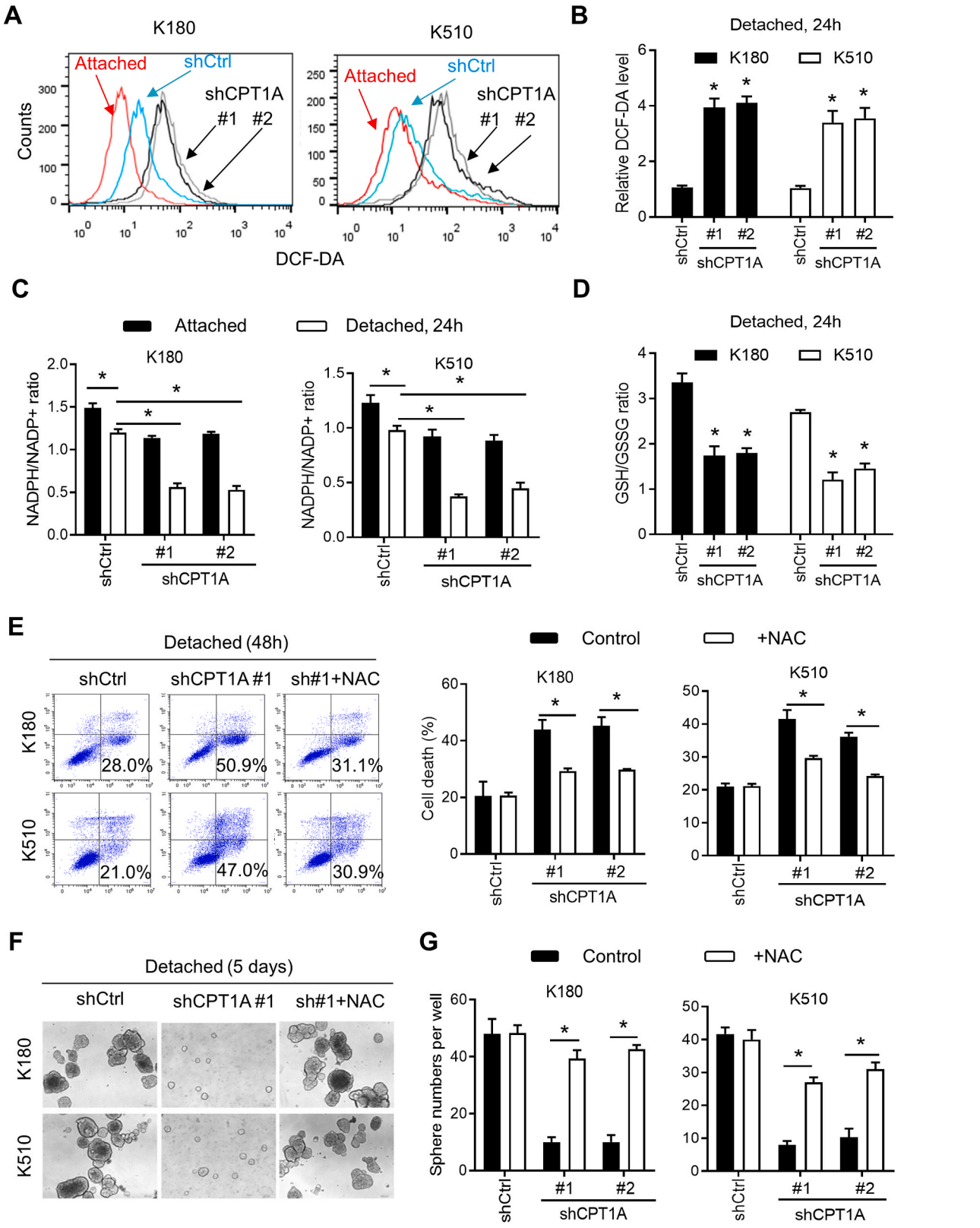

Fig. 3. Knockdown of CPT1A induced ROS stress of ESCC cells upon detached culture. **A.** DCF-DA analysis showing the ROS level in attached K180 and K510 cells (Red lines) and control (Blue lines) or CPT1A-knockdown (Gray and black lines) K180 and K510 cells after detached culture for 24 h. **B.** Quantification analysis of the ROS levels of control or CPT1A-knockdown K180 and K510 cells after detached culture for 24 h. **C, D.** NADPH/NADP+ (**C**) and GSS/GSSH (**D**) level assessment in control or CPT1A-knockdown K180 and K510 cells after attached or detached culture for 24 h. **E-G.** Apoptosis (Annexin V/PI staining) (**E**) and sphere formation (**F, G**) analysis in control or CPT1A-knockdown K180 and K510 cells after attached or detached culture with or without NAC (5 mM) treatment for 48 h and 5 days, respectively. Data in **B-D**, **E** and **G** are representative of three independent experiments and presented as mean ± S.D. The *P* values in **B-D**, **E** and **G** were calculated using two-sided unpaired Student's *t*-test. $^{*}P < 0.05$. (For interpretation of the references to color in this figure legend, the reader is referred to the Web version of this article.)

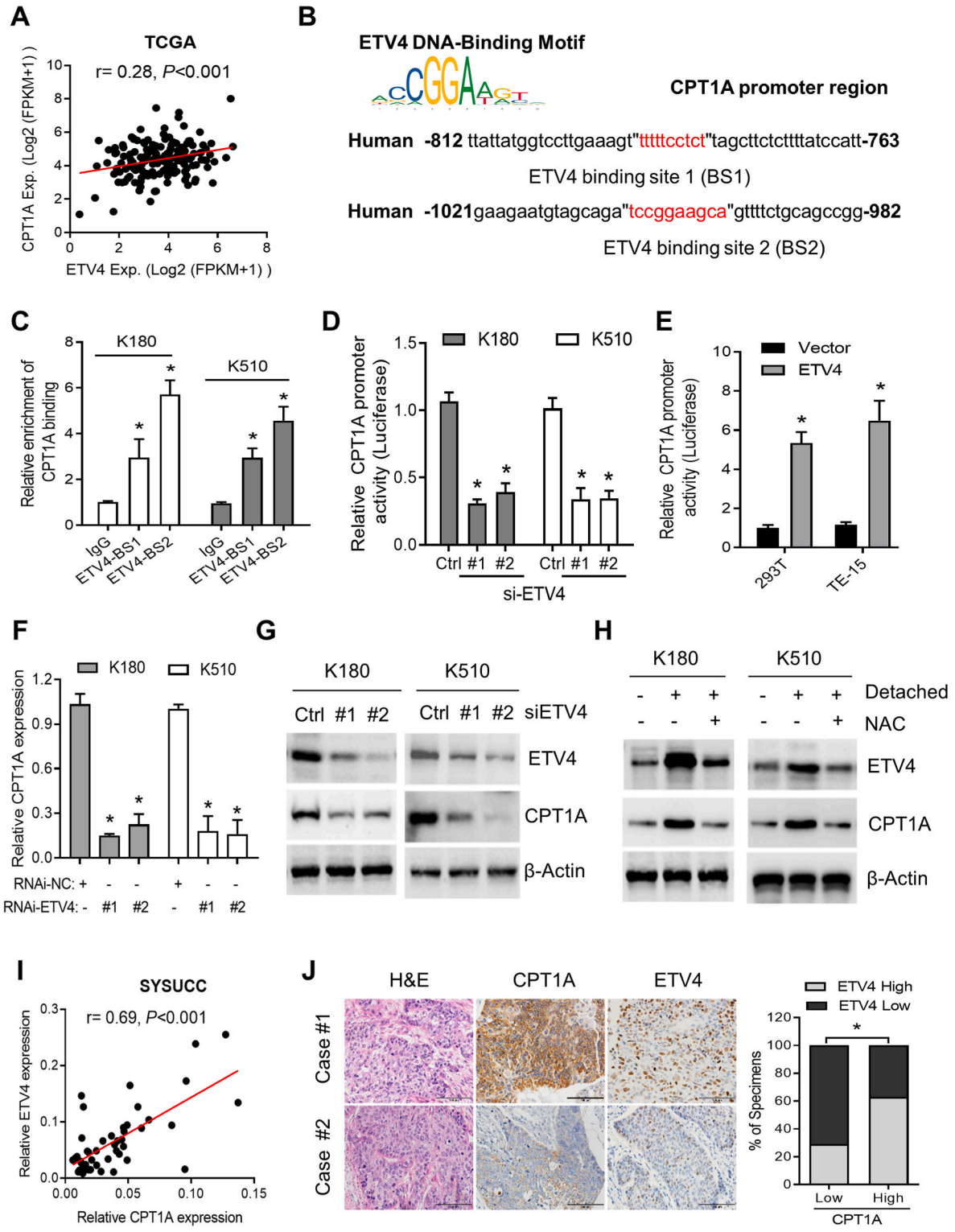

Fig. 4. ETV4 induced elevated expression of CPT1A of ESCC cells upon detached culture. **A.** Correlations between *CPT1A* expression and *ETV4* expression at the mRNA level based on the TCGA database. **B**. Schematic of the CPT1A promoter which contains two main ETV4 binding sites (BS1 and BS2). **C**. qPCR assay after ChIP analysis showing the occupancy of ETV4 binding sites on the CPT1A promoter (BS1 and BS2) in K180 and K510 cells. **D, E**. Luciferase promoter activity analysis of CPT1A transcriptional activity in cells silenced for ETV4 (K180 and K510 cells) (**D**) or overexpressing ETV4 (293T and TE-15 cells) (**E**). **F, G**. qPCR and Western blot analysis showing the CPT1A expression at the mRNA (**F**) and protein level (**G**) after silencing ETV4. **H**. Western blot analysis showing the expression of CPT1A and ETV4 after attached or detached culture with or without NAC (5 mM) treatment for 48 h. **I**. qPCR analysis in ESCC tumor tissues from SYSUCC showing that CPT1A expression is positively correlated with ETV4 expression (Pearson's correlation analysis). **J.** Representative IHC staining images showing CPT1A and ETV4 expression in ESCC tumor tissues from SYSUCC, scale bar = 100 μm (**left**); correlation between CPT1A expression and ETV4 expression based on the IHC scores (**right**). β-Actin was included as a loading control. Data in **C-F** are representative of three independent experiments and presented as mean ± S.D; data in **J** are presented as the percentage of total samples. The *P* values in **C-F** were calculated using two-sided unpaired Student's *t*-test, and those in **A** and **I** were calculated using Pearson's correlation analysis and chi-square test. $^*P < 0.05$.

collected clinical samples. At both the mRNA and protein levels, ETV4 and CPT1A showed a significantly positive association (Fig. 4I and J), validating their regulatory mechanisms. Altogether, overexpression of CPT1A in ESCC was regulated by ETV4 at the transcriptional level.

3.5. Ubiquitylation of CPT1A by RNF2 was suppressed by detachment culture

Post-translational modifications, such as ubiquitination, play central roles in maintaining protein stability. However, its roles in the regulation of CPT1A remain unsolved. When treated with CHX, a protein synthesis inhibitor, the expression of CPT1A was partially rescued under detached conditions (Fig. 5A), indicating that the mechanisms responsible for protein degradation may be involved in CPT1A regulation. Antibodies recognizing pan-ubiquitin suggested that the ubiquitylation of CPT1A was significantly suppressed in detached K180, K510 and TE11 cells (Fig. 5B). We then predicted the proteins that interact with CPT1A via the online databases and found that there are 6 ubiquitination-related proteins among them, including HERC2, FBXO6, RNF2, HUWE1, KBTBD7 and CACYBP (Supplementary Table S5). However, the protein expression of CPT1A was most significantly increased after silencing RNF2 but not the others (Fig. 5C and S2). RNF2 has been reported to enhance the radiosensitivity of ESCC[19]; therefore, we tested its roles in regulating CPT1A. Immunoprecipitation assays showed that CPT1A interacted with RNF2 in K180 and K510 cells (Fig. 5D). Knockdown of RNF2 significantly decreased the ubiquitin levels in K180 and K510 cells (Fig. 5E). Moreover, under detached culture conditions, the expression of RNF2 was suppressed in a time-dependent manner and showed an inverse tendency to that of CPT1A (Fig. 5F). IHC analysis showed that expression of RNF2 was downregulated in the liver metastases compared with primary cancer tissues (Fig. 5G). Expression of CPT1A and RNF2 showed negative correlations in clinical samples (Fig. 5G and H). In summary, the ubiquitin enzyme RNF2 was responsible for detachment induced CPT1A expression at the protein level.

3.6. Inhibition of CPT1A suppressed tumor metastasis in vivo

To further explore the *in vivo* functions of CPT1A, K180 cells with different CPT1A expression levels were injected into the tail vein of the mice, and lung metastase were monitored (Fig. 6A). Knockdown of CPT1A significantly suppressed lung metastatic nodules in both K180 and K510 cells (Fig. 6B). Moreover, perhexiline, a CPT1A inhibitor, reduced the CPTA1 activity *in vitro* (Figs. S3A and S3B) and showed antimetastatic roles *in vivo* (Fig. 6C and D), with no changes in the weight of the treated mice (Fig. 6E). The overall survival of mice treated with perhexiline was significantly longer than that of mice treated with PBS (Fig. 6F). Altogether, CPT1A promoted the lung metastasis *in vivo* and could be used as therapeutic target in ESCC.

4. Discussion

Esophageal cancer constituted approximately 535,000 new cancer cases and 498,000 deaths in 2019 worldwide [20], with more than 90% being the ESCC subtype and the most cases in Asian populations [21]. For patients with locally advanced ESCC, neoadjuvant chemoradiotherapy followed by surgery provided a median overall survival of more than 100 months and a 3-year survival rate of 69.1% [22]. However, the median overall survival was less than one year for patients whose tumor was inoperable or who had metastatic diseases [23–25]. Even when combined with an anti-PD1 antibody, chemotherapy remains the first-line mainstay for unresectable, advanced or metastatic ESCC with a limited overall survival ranging from 10 to 17 months [23–25]. Thus, uncovering molecular mechanisms underlying metastasis of ESCC and identifying therapeutic targets to inhibit the metastatic cascade are critical for improving overall survival.

During several different phases of metastasis including invasion into the nearby surroundings, floating in the circulation and extravasation into unfamiliar organs [3], only tumor cells that develop anoikis resistance can survive [4]. It was thus reasonable to speculate that the ability to evade anoikis upon detachment from the ECM determines to some extent the aggressiveness of tumor cells [3]. It has been reported that glycoproteins located in the cell membrane, such as ICAM1 are important for circulating tumor cells to form clusters with each other or other immune cells and thus provide a survival advantage [26]. Metabolic alteration is another route by which anoikis resistance develops and tumor metastases form [27]. The vulnerability to death of detached tumor cells may be exposed after elucidating the underlying metabolic mechanisms of anoikis resistance.

To survive harsh environments, including energy deprivation or detachment from the primary locus, tumor cells must rewire their metabolic flow to adapt to extracellular stress [1]. Although the Warburg effect or aerobic glycolysis has historically been the main focus of metabolic reprogramming of malignant cells, the lipogenic phenotype was recently identified as another metabolic hallmark of cancer [13]. Lipid rafts enriched in specific lipids can enable ESCC cells to metastasize to distant organs [28,29] and depletion of LPCAT1, which is responsible for cholesterol synthesis, has been shown to inhibit the anchorage-independent growth of ESCC cells [30]. We have previously reported that adipocyte predisposed metastatic addiction of gastric cancer cells into the peritoneum, while inhibition of the key enzyme DGAT2 responsible for the synthesis of triglycerides from diacylglycerol could block high fat diet induced anoikis resistance [10]. In contrast, less attention has been given to the catabolic side of lipid metabolism in cancer.

The fact that FAO plays central roles in providing mountainous ATP and NADPH in addition to glycolysis, especially in conditions of environmental stress such hypoxia, glucose deprivation or detachment has received much attention in the last decade [31]. Understanding precisely how FAO facilitates tumor progression will provide novel insights into how early cancers develop into the metastatic stage or whether imposed metabolic programs could be exploited therapeutically [31]. Aberrant activation of the FAO pathways has been reported in breast cancer [11] and ovarian cancer [15,32], and overexpression of key enzymes was associated with chemoresistance, stemness and metastasis [11,14,15,33]. The oncogenic roles and therapeutic exploitation of CPT1A have been widely studied in several forms of cancer, including ovarian cancer [15], breast cancer [11] and colorectal cancer [8].

Another aspect where CPT1A also contributes to cancer cell survival is anoikis resistance [8], which is necessary for metastasis. We previously found that CPT1A-mediated fat oxidation increased metastatic capacity and anoikis resistance in colorectal cancer cells [8]. Furthermore, in clinical samples, we found increased expression of CPT1A in metastatic sites compared with primary sites, suggesting that CPT1A could be an attractive target for metastatic colon cancer [8]. Another cancer in which CPT1A promotes anoikis resistance is high-grade serous ovarian cancer (HGSOC) [15]. Previous studies have identified that CPT1A-mediated FAO is vital for cell cycle progression, anchorage-independent growth [32], and resistance to platinum [15] and suggested that CPT1A could be a prognostic biomarker and therapeutic target in ovarian cancer patients [15,32]. Moreover, we identified for the first time the transcription factor and ubiquitin enzyme responsible for elevated expression of CPT1A upon detachment, underscoring the complexity of CPT1A regulation in different contexts.

Of course, our study does have some limitations. First, other enzymes involved in NADPH generation such as ME1(17),G6PD(7) or MTHFD2 (9), as reported in our previous studies, were not upregulated in detached ESCC cells, which reflects tumor type dependent metabolic reprogramming upon detached stress. Second, clinical trials testing CPT1A inhibitors were suspended due to adverse events, which warrants further investigation before they are clinically available.

Our results showed that upon detached stress, overexpression of

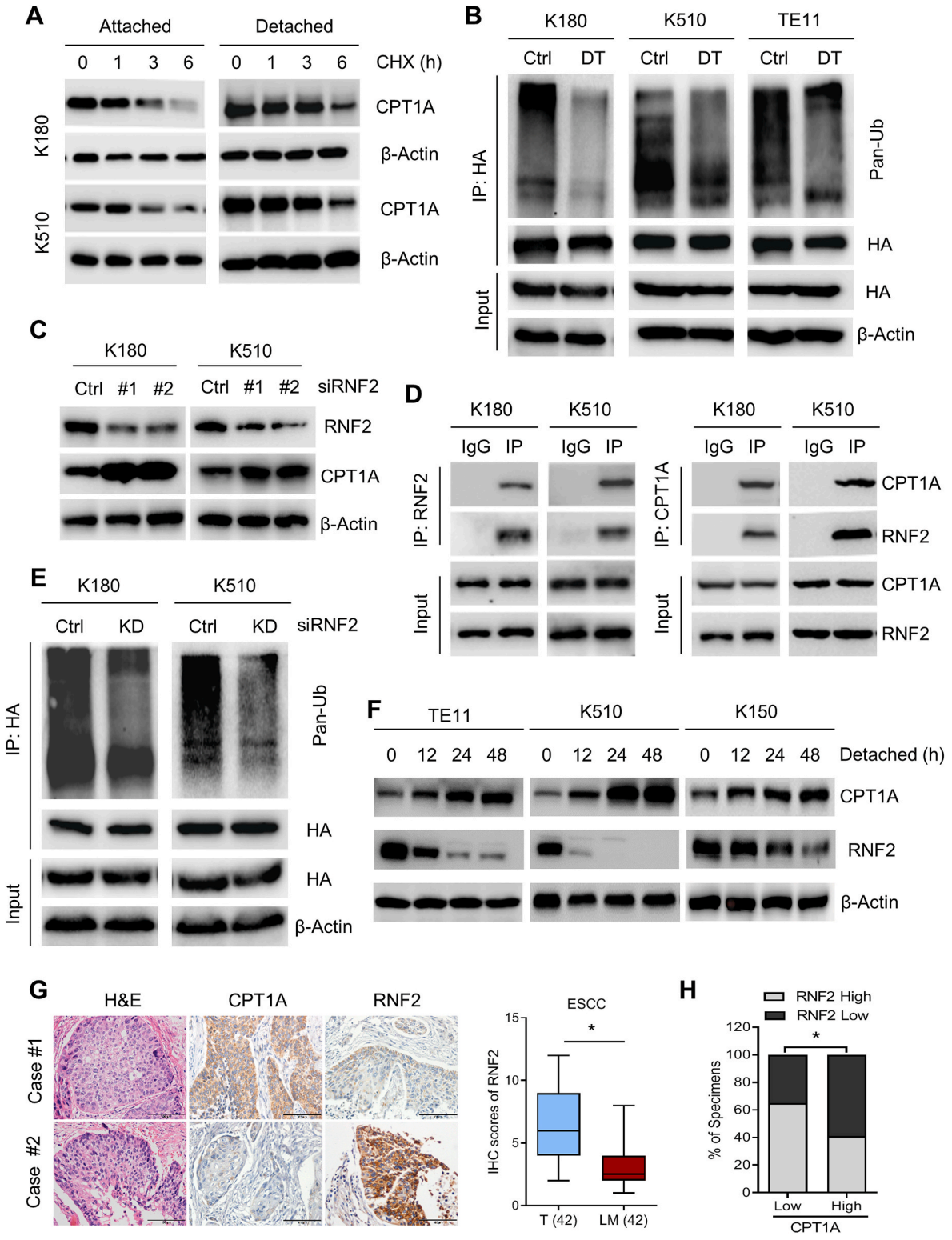

Fig. 5. RNF2 mediated ubiquitination of CPT1A was suppressed upon detached culture in ESCC cells. **A**. Western blot analysis of CPT1A expression in K180 and K510 cells treated with CHX for 1 h, 3 h and 6 h. **B**. IP analysis demonstrating the ubiquitination (Pan-Ub) level of CPT1A in K180, K510 and TE11 cells after attached or detached culture for 24h. **C**. Western blot analysis of CPT1A and RNF2 expression in control and RNF2-knockdown K180 and K510 cells. **D**. IP analysis demonstrating the interaction between CPT1A and RNF2. **E**. IP analysis showing the ubiquitination (Pan-Ub) level of CPT1A in control and RNF2-knockdowned K180 and K510 cells. **F**. Western blot analysis of CPT1A and RNF2 expression after attached or detached culture for 12 h, 24h, 48 h. **G**. Representative IHC staining images showing CPT1A and RNF2 expression **(left)** and the IHC score of RNF2 **(right)** in ESCC tumor tissues from SYSUCC. Scale bar = 100 μm. **H**. Correlation between CPT1A expression and RNF2 expression. β-Actin was included as a loading control. Data in **G** are presented as a box-and-whiskers graph (min-max), and the horizontal line across each box indicates the median; data in **H** are presented as the percentage of total samples. The *P* values in **G** were calculated using two-sided paired Student's *t*-test and those in **H** were calculated using Pearson's correlation analysis and chi-square test. $^{*}P < 0.05$.

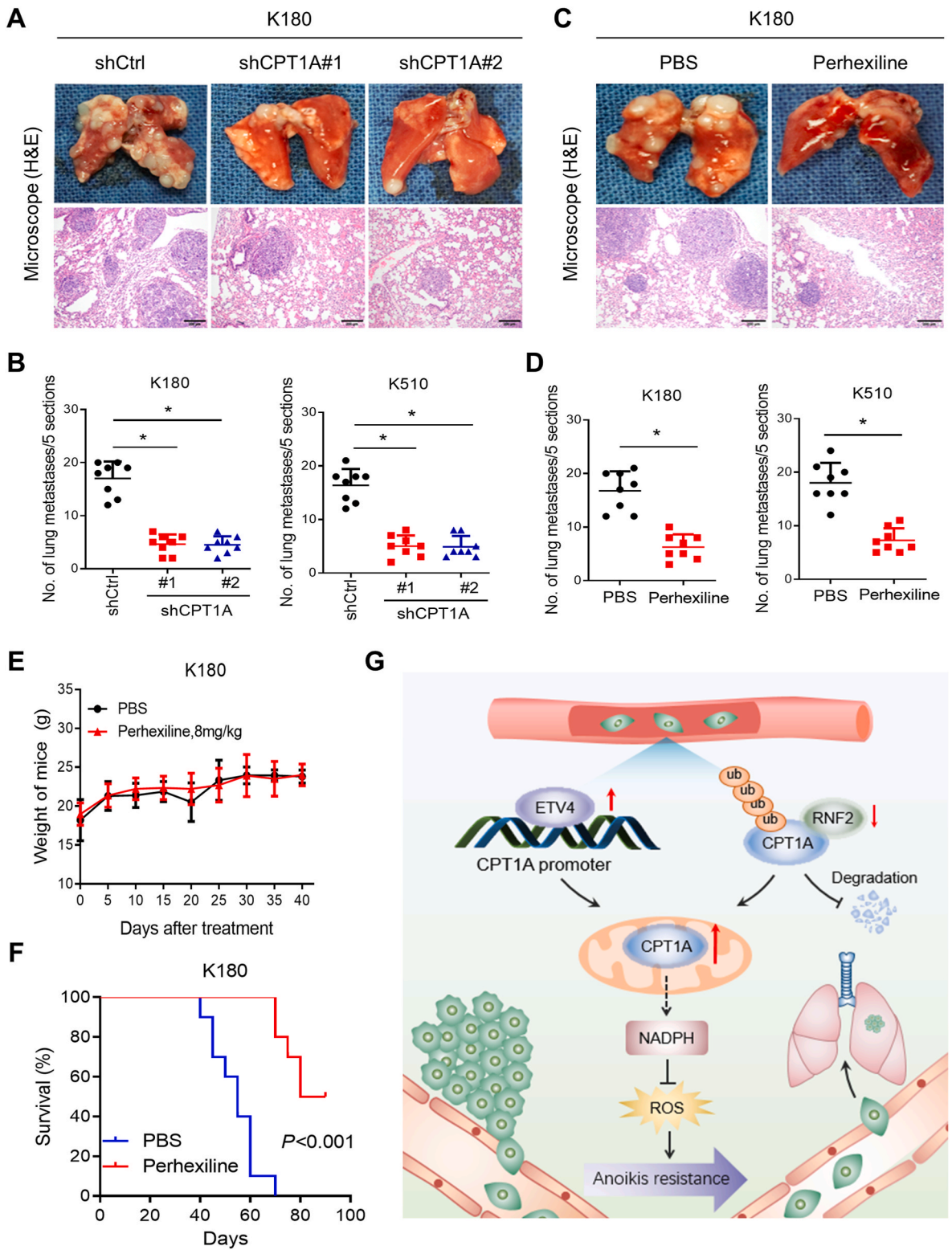

Fig. 6. Inhibition of CPT1A suppressed lung metastasis of CDX *in vivo*. **A, B.** Representative images and H&E staining (**A**) and statistical results of metastatic lung nodules (**B**) from mice injected via the tail vein with CPT1A knockdown and control K180 and K510 cells (five sections evaluated per lung). **C, D**. Representative images and H&E staining (**C**) and statistical results of metastatic lung nodules (**D**) from mice injected via the tail vein with PBS and CPT1A inhibitor (perhexiline, 8 mg/kg) treatment (five sections evaluated per lung). **E, F**. The weight (**E**) and survival (**F**) analysis of K180 cell–based CDX mice model with PBS and CPT1A inhibitor (perhexiline, 8 mg/kg) treatment. **G**. Proposed working model of this study. The *P* values in **B** and **D** were calculated using two-sided unpaired Student's *t*-test and those in **F** using Kaplan-Meier analysis with the log-rank test. $^{*}P < 0.05$.

CPT1A could protect ESCC cells from apoptosis by maintaining redox homeostasis through the supply of GSH and NADPH. Mechanistically, the transcription factor ETV4 and the ubiquitin enzyme RNF2 were responsible for the elevated expression of CPT1A upon detachment at the mRNA and protein levels, respectively. Moreover, the expression of CPT1A was positively associated with ETV4 and negatively associated with RNF2. Overexpression of CPT1A was found in ESCC cancer tissues compared with normal tissues and predicted poor overall and disease-free survival of ESCC. Most importantly, genetic or pharmacologic disruption of CPT1A switched off the NADPH supply via FAO and therefore prevented cell proliferation of ESCC cells *in vitro* and lung metastasis of orthotopic xenograft tumor models *in vivo* (Fig. 6G). Collectively, our results provide novel insights into how ESCC cancer cells exploit metabolic switching to form distant metastases and add preclinical evidence and rationale that support further investigation of FAO as a potential therapeutic opportunity for the treatment of ESCC.

5. Availability of data and materials

The other datasets used and/or analyzed during the current study are available from the corresponding author upon reasonable request.

Authors' contributions

Conceptualization, WGD, TT, HY and JSH; Methodology, TT, YXL, JFL, MC, HJQ, WCZ, HHS, JSH and HY; Investigation, TT, YXL, JFL, MC, HJQ, WCZ, HHS, JSH and HY; Writing-Original Draft, TT and YXL; Writing–Review & Editing, WGD, TT and HY; Funding Acquisition, TT, YXL and WGD; Supervision, WGD and JSH.

Declaration of competing interest

The authors declare no conflicts of interest.

Data availability

Data will be made available on request.

Acknowledgments

This research was supported by National Natural Science Foundation of China (82203732, 81972569, 82172949, 82002465), the Natural Science Foundation of Guangdong Grant (2022A1515012508), the China Postdoctoral Science Foundation (2022M711336) and Open Funds of State Key Laboratory of Oncology in South China (HN2022-06).

Appendix A. Supplementary data

Supplementary data to this article can be found online at https://doi.org/10.1016/j.redox.2022.102544.

References

[1] F. Weiss, D. Lauffenburger, P. Friedl, Towards targeting of shared mechanisms of cancer metastasis and therapy resistance, Nat. Rev. Cancer 22 (2022) 157–173.
[2] A. Rogiers, I. Lobon, L. Spain, S. Turajlic, The genetic evolution of metastasis, Cancer Res. 82 (2022) 1849–1857.
[3] S.U. Khan, K. Fatima, F. Malik, Understanding the cell survival mechanism of anoikis-resistant cancer cells during different steps of metastasis, Clin. Exp. Metastasis (2022).
[4] Z.T. Schafer, A.R. Grassian, L. Song, Z. Jiang, Z. Gerhart-Hines, H.Y. Irie, et al., Antioxidant and oncogene rescue of metabolic defects caused by loss of matrix attachment, Nature 461 (2009) 109–113.
[5] S.M. Jeon, N.S. Chandel, N. Hay, AMPK regulates NADPH homeostasis to promote tumour cell survival during energy stress, Nature 485 (2012) 661–665.
[6] Y.N. Wang, Y.X. Lu, J. Liu, Y. Jin, H.C. Bi, Q. Zhao, et al., AMPKalpha1 confers survival advantage of colorectal cancer cells under metabolic stress by promoting redox balance through the regulation of glutathione reductase phosphorylation, Oncogene 39 (2020) 637–650.
[7] H.Q. Ju, Y.X. Lu, Q.N. Wu, J. Liu, Z.L. Zeng, H.Y. Mo, et al., Disrupting G6PD-mediated Redox homeostasis enhances chemosensitivity in colorectal cancer, Oncogene 36 (2017) 6282–6292.
[8] Y.N. Wang, Z.L. Zeng, J. Lu, Y. Wang, Z.X. Liu, M.M. He, et al., CPT1A-mediated fatty acid oxidation promotes colorectal cancer cell metastasis by inhibiting anoikis, Oncogene 37 (2018) 6025–6040.
[9] H.Q. Ju, Y.X. Lu, D.L. Chen, Z.X. Zuo, Z.X. Liu, Q.N. Wu, et al., Modulation of redox homeostasis by inhibition of MTHFD2 in colorectal cancer: mechanisms and therapeutic implications, J. Natl. Cancer Inst. 111 (2019) 584–596.
[10] S. Li, T. Wu, Y.X. Lu, J.X. Wang, F.H. Yu, M.Z. Yang, et al., Obesity promotes gastric cancer metastasis via diacylglycerol acyltransferase 2-dependent lipid droplets accumulation and redox homeostasis, Redox Biol. 36 (2020), 101596.
[11] N. Jariwala, G.A. Mehta, V. Bhatt, S. Hussein, K.A. Parker, N. Yunus, et al., CPT1A and fatty acid beta-oxidation are essential for tumor cell growth and survival in hormone receptor-positive breast cancer, NAR cancer 3 (2021) zcab035.
[12] C. Corbet, E. Bastien, J.P. Santiago de Jesus, E. Dierge, R. Martherus, C. Vander Linden, et al., TGFbeta2-induced formation of lipid droplets supports acidosis-driven EMT and the metastatic spreading of cancer cells, Nat. Commun. 11 (2020) 454.
[13] C. Zhang, N. Zhu, H. Li, Y. Gong, J. Gu, Y. Shi, et al., New dawn for cancer cell death: emerging role of lipid metabolism, Mol. Metabol. 63 (2022), 101529.
[14] M. Tang, X. Dong, L. Xiao, Z. Tan, X. Luo, L. Yang, et al., CPT1A-mediated fatty acid oxidation promotes cell proliferation via nucleoside metabolism in nasopharyngeal carcinoma, Cell Death Dis. 13 (2022) 331.
[15] D. Huang, S. Chowdhury, H. Wang, S.R. Savage, R.G. Ivey, J.J. Kennedy, et al., Multiomic analysis identifies CPT1A as a potential therapeutic target in platinum-refractory, high-grade serous ovarian cancer, Cell Rep. Med. 2 (2021), 100471.
[16] B. Raud, D.G. Roy, A.S. Divakaruni, T.N. Tarasenko, R. Franke, E.H. Ma, et al., Etomoxir actions on regulatory and memory T cells are independent of Cpt1a-mediated fatty acid oxidation, Cell Metabol. 28 (2018) 504–515 e7.
[17] Y.X. Lu, H.Q. Ju, Z.X. Liu, D.L. Chen, Y. Wang, Q. Zhao, et al., ME1 regulates NADPH homeostasis to promote gastric cancer growth and metastasis, Cancer Res. 78 (2018) 1972–1985.
[18] Y. Wang, J.H. Lu, F. Wang, Y.N. Wang, M.M. He, Q.N. Wu, et al., Inhibition of fatty acid catabolism augments the efficacy of oxaliplatin-based chemotherapy in gastrointestinal cancers, Cancer Lett. 473 (2020) 74–89.
[19] J. Yang, F. Yu, J. Guan, T. Wang, C. Liu, Y. Wang, et al., Knockdown of RNF2 enhances the radiosensitivity of squamous cell carcinoma in lung, Biochem. Cell Biol. = Biochimie et biologie cellulaire 97 (2019) 589–599.
[20] C. Global Burden of Disease Cancer, J.M. Kocarnik, K. Compton, F.E. Dean, W. Fu, B.L. Gaw, et al., Cancer incidence, mortality, years of life lost, years lived with disability, and disability-adjusted life years for 29 cancer groups from 2010 to 2019: a systematic analysis for the global burden of disease study 2019, JAMA Oncol. 8 (2022) 420–444.
[21] G.B.D.O.C. Collaborators, The global, regional, and national burden of oesophageal cancer and its attributable risk factors in 195 countries and territories, 1990-2017: a systematic analysis for the Global Burden of Disease Study 2017, Lancet Gastroenterol. Hepatol. 5 (2020) 582–597.
[22] H. Yang, H. Liu, Y. Chen, C. Zhu, W. Fang, Z. Yu, et al., Neoadjuvant chemoradiotherapy followed by surgery versus surgery alone for locally advanced squamous cell carcinoma of the esophagus (NEOCRTEC5010): a phase III Multicenter, randomized, open-label clinical trial, J. Clin. Oncol. 36 (2018) 2796–2803.
[23] J.M. Sun, L. Shen, M.A. Shah, P. Enzinger, A. Adenis, T. Doi, et al., Pembrolizumab plus chemotherapy versus chemotherapy alone for first-line treatment of advanced oesophageal cancer (KEYNOTE-590): a randomised, placebo-controlled, phase 3 study, Lancet 398 (2021) 759–771.
[24] Y. Doki, J.A. Ajani, K. Kato, J. Xu, L. Wyrwicz, S. Motoyama, et al., Nivolumab combination therapy in advanced esophageal squamous-cell carcinoma, N. Engl. J. Med. 386 (2022) 449–462.
[25] Z.X. Wang, C. Cui, J. Yao, Y. Zhang, M. Li, J. Feng, et al., Toripalimab plus chemotherapy in treatment-naive, advanced esophageal squamous cell carcinoma (JUPITER-06): a multi-center phase 3 trial, Cancer Cell 40 (2022) 277–288 e3.
[26] R. Taftaf, X. Liu, S. Singh, Y. Jia, N.K. Dashzeveg, A.D. Hoffmann, et al., ICAM1 initiates CTC cluster formation and trans-endothelial migration in lung metastasis of breast cancer, Nat. Commun. 12 (2021) 4867.
[27] F.A. Urra, S. Fuentes-Retamal, C. Palominos, Y.A. Rodriguez-Lucart, C. Lopez-Torres, R. Araya-Maturana, Extracellular matrix signals as drivers of mitochondrial bioenergetics and metabolic plasticity of cancer cells during metastasis, Front. Cell Dev. Biol. 9 (2021), 751301.
[28] J.D. Greenlee, T. Subramanian, K. Liu, M.R. King, Rafting down the metastatic cascade: the role of lipid rafts in cancer metastasis, cell death, and clinical outcomes, Cancer Res. 81 (2021) 5–17.
[29] H. Gong, L. Song, C. Lin, A. Liu, X. Lin, J. Wu, et al., Downregulation of miR-138 sustains NF-kappaB activation and promotes lipid raft formation in esophageal squamous cell carcinoma, Clin. Cancer Res. : an official journal of the American Association for Cancer Research 19 (2013) 1083–1093.
[30] M. Tao, J. Luo, T. Gu, X. Yu, Z. Song, Y. Jun, et al., LPCAT1 reprogramming cholesterol metabolism promotes the progression of esophageal squamous cell carcinoma, Cell Death Dis. 12 (2021) 845.

[31] I.R. Schlaepfer, M. Joshi, CPT1A-mediated fat oxidation, mechanisms, and therapeutic potential, Endocrinology (2020) 161.
[32] B.T. Sawyer, L. Qamar, T.M. Yamamoto, A. McMellen, Z.L. Watson, J.K. Richer, et al., Targeting fatty acid oxidation to promote anoikis and inhibit ovarian cancer progression, Mol. Cancer Res. : MCR 18 (2020) 1088–1098.
[33] M.D. Mana, A.M. Hussey, C.N. Tzouanas, S. Imada, Y. Barrera Millan, D. Bahceci, et al., High-fat diet-activated fatty acid oxidation mediates intestinal stemness and tumorigenicity, Cell Rep. 35 (2021), 109212.